

A role for hydrophobic residues in the voltage-dependent gating of Shaker K⁺ channels

(ion channels/leucine heptad repeat/leucine zipper/4-aminopyridine)

KEN McCORMACK*, MARK A. TANOUYE*†, LINDA E. IVERSON‡, JEN-WEI LIN§, MANI RAMASWAMI*†, TOM McCORMACK§, JAMES T. CAMPANELLI*, MATHEW K. MATHEW*†, AND BERNARDO RUDY§

*Division of Biology 216-76, California Institute of Technology, Pasadena, CA 91125; †Division of Neurosciences, Beckman Research Institute, City of Hope, Duarte, CA 91010; and §Department of Physiology and Biophysics and Department of Biochemistry, New York University Medical Center, 550 1st Avenue, New York, NY 10016

Communicated by Norman Davidson, January 7, 1991

ABSTRACT A leucine heptad repeat is well conserved in voltage-dependent ion channels. Herein we examine the role of the repeat region in Shaker K⁺ channels through substitution of the leucines in the repeat and through coexpression of normal and truncated products. In contrast to leucine-zipper DNA-binding proteins, we find that the subunit assembly of Shaker does not depend on the leucine heptad repeat. Instead, we report that substitutions of the leucines in the repeat produce large effects on the observed voltage dependence of conductance voltage and prepulse inactivation curves. Our results suggest that the leucines mediate interactions that play an important role in the transduction of charge movement into channel opening and closing.

The Shaker gene family (*Sh*) encodes proteins that produce voltage-dependent K⁺-selective currents (1-3). Like other voltage-dependent ion channels, Sh channels open and close an aqueous pore by undergoing conformational transitions in response to changes in membrane potential. This gating behavior includes the movement of a charged component or voltage sensor (4, 5). Interestingly, mutagenesis of charged residues in the S4 domain (a proposed transmembrane segment that contains four to eight basic residues and is found in virtually all voltage-dependent ion channels including Sh) of the rat II Na⁺ channel showed that it exhibits some of the properties expected for a voltage sensor (6). However, the voltage-dependent gating mechanism remains unclear; in particular, it is not known how movement of the voltage sensor(s) is transduced into the conformational transitions that result in opening and closing of the channel pore.

Functional Sh channels are likely to be tetramers since Na⁺ and Ca²⁺ channels are composed of four homology domains, each roughly equivalent to a single K⁺ channel subunit (7). Although recent work has shown that Sh channels are multimeric (8), the sites of subunit interaction are unknown. Sh channels contain a conserved leucine heptad repeat (five leucines long) that overlaps two proposed transmembrane segments (S4 and S5); similar motifs are found in Na⁺ and Ca²⁺ channels (9) (Fig. 1). Ion-channel leucine heptad repeats are preceded by, and partially overlap, the basic S4 domain (Fig. 1). DNA-binding leucine-zipper proteins also contain a basic (DNA binding) domain preceding a leucine heptad repeat. Mutational analyses of the DNA-binding proteins have shown that leucines within the heptad repeat play a primary role in the dimerization of subunits and juxtaposition of the basic DNA-binding domains (13, 14). The functional significance of similar sequences reported in other proteins is unknown (9, 15, 16).

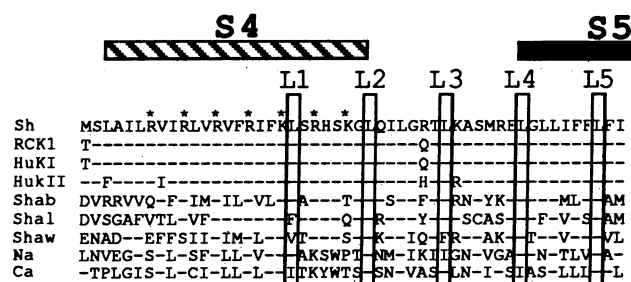


FIG. 1. Deduced amino acid alignments of the leucine-heptad-repeat region. Basic residues in S4 (stars) and leucine residues in the heptad repeat (boxed) were aligned. Amino acids identical to Sh are indicated by dashes. Proposed transmembrane segments S4 and S5 are indicated. Sh (10) is the *Drosophila* Shaker channel. Other K⁺ channel sequences are a rat Sh homolog (RCK1) (2), two human Sh homologs (Huk1 and Huk2) (11), and Shab, Shaw, and Shal, which represent other *Drosophila* K⁺ channel genes (3). Na and Ca sequences are from the second homology domains of the rat IIa Na⁺ channel and the skeletal muscle dihydropyridine receptor (12), respectively.

Since Sh K⁺ channels are multimeric it suggests that the leucine heptad repeat might act as a site for subunit assembly. In addition, the close proximity of the repeat to the S4 domain suggests that the voltage sensor may introduce a voltage dependence to the interactions mediated by residues in the leucine-heptad-repeat region; gating may be a process involving the dynamics of these interactions (9). With this in mind we attempted to determine the role of the conserved leucine residues in (i) channel assembly and (ii) voltage-dependent gating.

MATERIALS AND METHODS

Mutants. The S4x and 102 truncations were full-length 29-4 cDNAs (10, 17) with stop codons at positions Ile-360 and Trp-422, respectively. E1 contains a stop codon at position Lys-320 and no downstream coding sequence (10). V1n-3 is a valine substitution at position Ile-360. Other substitutions are at Leu-363, -370, -377, -384, and -391, corresponding to L1-L5, respectively. All constructs were sequenced to verify the appropriate changes.

RNA Synthesis and Expression. *In vitro* RNA transcripts were prepared from cDNA templates and injected into *Xenopus* oocytes, and macroscopic currents were recorded using a standard two-microelectrode voltage clamp as de-

Abbreviations: 4-AP, 4-aminopyridine; $V_{m1/2}$, voltage of half-maximal conductance; $V_{h1/2}$, voltage of half steady-state inactivation.

†Present address: Department of Entomology, 201 Wellman Hall, University of California, Berkeley, CA 94720.

scribed by Iverson *et al.* (1). Currents were low-pass filtered at 3 kHz. Voltage and current records were digitized and analyzed using the pCLAMP system. A 1 M 4-aminopyridine (4-AP; Sigma) stock solution was made fresh and dilutions to the appropriate concentrations were adjusted to pH 7.5 prior to use. Tetrodotoxin was kept frozen at 500 μ M and diluted prior to use.

RESULTS

Role of the Leucine-Heptad-Repeat Region in Subunit Assembly. To determine if the leucine repeat region acts as a primary site for the association of subunits, we coinjected normal *Drosophila* Shaker (Sh) RNA, 29-4 (17), with several RNAs encoding truncated 29-4 proteins (Fig. 2) into *Xenopus* oocytes. A truncated nonfunctional Sh product (Sh¹⁰²) appears to associate with normal subunits and inhibit their

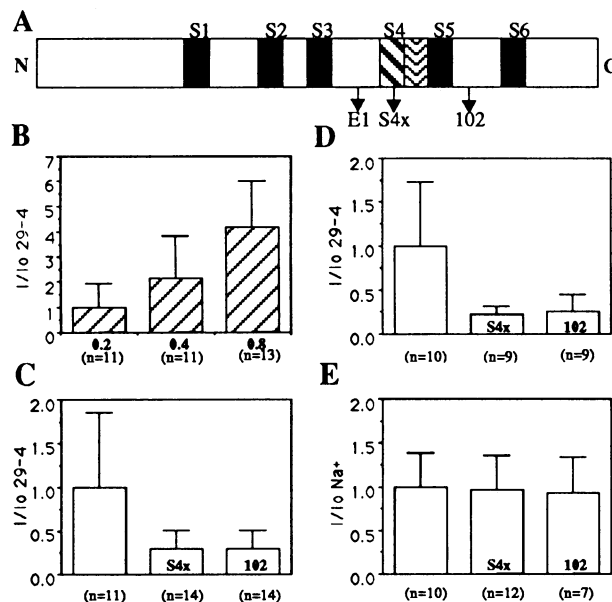


FIG. 2. (A) Schematic diagram of a Sh subunit. S1–S6 denote potential membrane-spanning segments; the leucine heptad repeat overlaps S4 and S5. The locations of E1, S4x, and Sh¹⁰² (102) C-terminal truncations are indicated. (B) Normalized currents of 29-4 (I/I_0) at the indicated concentrations of RNA (ng per oocyte). Expression of currents is linear over the concentration ranges examined; the ability of the oocytes to translate and assemble Sh 29-4 products is apparently not limiting at these concentrations. (C) Oocytes were injected with 29-4 RNA (0.2 ng) alone or coinjected with 29-4 (0.2 ng) and the indicated truncated (0.4 ng) RNA (S4x or 102). The truncated RNAs eliminated about 70% of the expressed 29-4 current. The S4x and 102 truncations inhibited 29-4 currents equally well; similar results were seen with coinjections of E1 (data not shown). No alterations were seen in voltage-dependent or kinetic behavior for the currents expressed in coinjected oocytes. In D and E, we demonstrate that the inhibitory effects of the truncations are specific to the 29-4 currents; Na⁺ channel expression is unaffected. (D) Coinjection of 29-4 (0.25 ng) plus rat IIa Na⁺ channel (1.0 ng) RNAs or 29-4 (0.25 ng), rat IIa Na⁺ channel (1.0 ng), plus the indicated truncated (0.50 ng) RNA (S4x or 102). Recordings were made in the presence of 500 nM tetrodotoxin to block Na⁺ currents. Truncated RNA inhibited the tetrodotoxin-insensitive current by about 75%. (E) Similar experiment to D but the oocytes were recorded from in the presence of 4 mM 4-AP to block Sh currents. These data suggest that the truncated products specifically associate with Sh subunits. All currents were leak-subtracted (17) and normalized to currents obtained when no truncations were injected. All experiments were done on the same batch of oocytes 3 days after injection and within an 8-hr period. Oocytes were held at -90 and stepped to $+70$ mV for 29-4 and -10 mV for rat IIa (M860) currents. All data are mean \pm SD.

functional expression (18, 19). The Sh¹⁰² truncation occurs downstream of the leucine heptad repeat: our truncated constructs contained stop codons at sites before (E1 or S4x) or after (Sh¹⁰²) the leucine heptad repeat (Fig. 2). As shown, Sh products truncated before and after the zipper region inhibit 29-4 expression equally well. This suggests that the assembly of Sh subunits is not dependent on the leucine heptad motif, in contrast to the role seen for similar sequence motifs in DNA-binding proteins. Furthermore, our results suggest that a primary site for subunit assembly lies in a region prior to the S4 segment.

Role of the Leucines in the Heptad Repeat in Voltage-Dependent Gating. Leucines in the heptad repeat (L1, L2, L3, L4, and L5) were switched individually to valine (the V1, V2, V3, V4, and V5 mutants), alanine (A3), or both valine and alanine (V2A3). As a control, an isoleucine in S4, three residues upstream of L1, was switched to valine (V1n-3) (see Fig. 1). All of the mutants examined expressed well and showed similar ion selectivity (data not shown) and general kinetic behavior (see below), indicating that none of the substitutions caused gross alteration of the native channel structure.

Typical currents observed in *Xenopus* oocytes injected with 29-4 and mutant RNA are illustrated in Fig. 3. The 29-4 currents display properties similar to those reported previously (17). The V2 and V4 mutants also produce currents with transient A-type kinetics. However, V2 currents are observed only at potentials much more positive than those necessary to activate 29-4 currents whereas the V4 mutation has the opposite effect: V4 currents are observed at potentials more negative than those seen for 29-4. Normalized conductance–voltage relations (Fig. 3D) show that the voltages at which conductance reaches half-maximal value ($V_{m1/2}$) is shifted about $+70$ mV for V2 and -25 mV for V4. The V1 mutation produces a depolarizing shift like that of V2 but of larger magnitude, whereas the conductance–voltage curves of V3 and V5 are shifted in the same direction as V4 (Table 1). Shifts in voltage dependence for substitutions of L3 appear to be due to the degree of hydrophobicity, or the chain length, rather than steric constraints since an alanine substitution (A3) causes a larger voltage shift than V3. The observed shifts in the conductance–voltage curves suggest that the leucines play an important role in determining the relative stabilities of open and closed states of the channel. In addition, all of the leucine substitutions have parallel shifts in the prepulse inactivation curves (Fig. 3E and Table 1), supporting the hypothesis that inactivation is coupled to channel opening (20).

To test the possibility of alterations in the closed states of mutant channels, we examined the sensitivity of two of the mutants to the state-dependent K⁺ channel blocker/4-AP, which appears to bind preferentially to channels in the closed state (21, 22). V2 currents are more sensitive whereas V4 currents are more than two orders of magnitude less sensitive than the wild-type currents (Fig. 2F). Although it is possible that these differences may be due to modifications in the binding site for 4-AP, they are consistent with increased and reduced lifetimes for closed states in the V2 and V4 mutants, respectively. In particular, the large decrease in 4-AP sensitivity in V4 channels may indicate that a closed state(s) that preferentially binds 4-AP is very short lived in these channels.

Both the V1 and V2 currents show dramatic decreases in the slopes of the conductance–voltage and prepulse inactivation curves. Mutations of the other heptad leucines (V3, A3, V4, and V5) cause little apparent change in slope (Fig. 3 and Table 1). Since the slope of the steady-state inactivation curve has been suggested to be a better indicator for the number of charges moved during the activation process in Sh currents (20), the apparent number of “gating charges” is

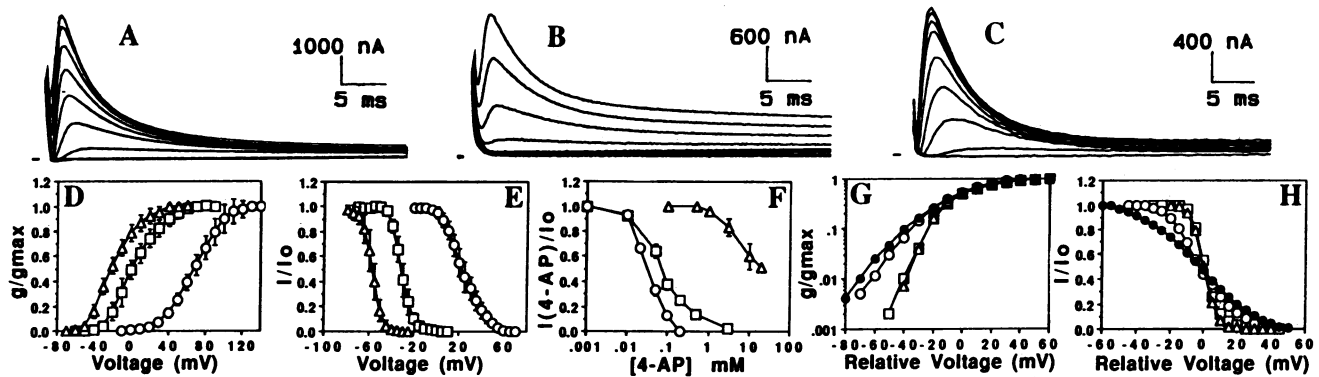


FIG. 3. Macroscopic currents from a *Xenopus* oocyte injected with 29-4 (A), V2 (B), or V4 (C) RNA. Oocytes were held at -90 mV, stepped to a -120 -mV prepulse for 1 s, and then depolarized from -60 to 100 mV in 20 -mV increments. The time between episodes was 10 s. Only the currents during the depolarizing pulses are shown. For D–H, the following symbols are used for 29-4 (open squares), V4 (open triangles), V2 (open circles), and V1 (solid circles) currents. (D) A similar protocol (above) but in 10 -mV increments was used to plot conductance–voltage relations. Conductance was determined by $g = I_p / (V - V_k)$ where I_p is the peak current at voltage V , and V_k , the K^+ equilibrium potential, is taken as -90 mV. Conductances were normalized (g/g_{max}) by dividing the conductance at the indicated potential by the maximum observed conductance. Currents (I_p) were obtained after leak subtraction (17). Data are mean \pm SD, where $n = 15, 7,$ and 5 for 29-4, V2, and V4, respectively. (E) Normalized prepulse inactivation. Oocytes were held at -100 mV, stepped for 500 ms to the indicated prepulse voltages, and then depolarized to a test pulse of 30 (29-4 and V4) or 80 mV (V2). The time between episodes was 10 s. Peak currents obtained during the test pulse after a prepulse to the indicated voltage were divided by the peak currents obtained during a test pulse after a prepulse to -80 mV. Data are mean \pm SD, where $n = 9, 4,$ and 4 for 29-4, V2, and V4, respectively. (F) 4-AP sensitivities of 29-4, V2, and V4. 4-AP was continuously circulated through the recording chamber. The effect of 4-AP was monitored with a series of voltage steps (1 /min) until no further change was observed (usually 5 – 10 min). The peak currents at 20 mV (29-4 and V4) or 70 mV (V2) at the indicated concentrations of 4-AP were divided by the peak currents at the same voltage in the absence of 4-AP. Data are mean \pm SD, where $n = 4, 4,$ and 5 for 29-4, V2, and V4, respectively. (G) The logarithm of the normalized conductance (cf. D) of the indicated Sh constructs. To facilitate comparisons of slope, relative voltages are used, with $V_{m1/2}$ for each construct taken as 0 mV. All values are the mean, where $n = 15, 5, 7,$ and 5 for 29-4, V1, V2, and V4, respectively. (H) Steady-state inactivation relationships for the indicated constructs (cf. Fig. 2E). To facilitate comparisons of slope, the voltage of half steady-state inactivation ($V_{h1/2}$), is defined as 0 mV for each of the constructs. All values are the mean where $n = 9, 4, 4,$ and 4 for 29-4, V1, V2, and V4, respectively.

calculated from this slope in Table 1. The total apparent gating charge of a 29-4 channel is ≈ 7 whereas it is reduced ≈ 3 -fold for V2 and 5-fold for V1.

As in previous reports of Sh currents (17), 29-4 and the mutant currents exhibit a rapidly inactivating and a noninactivating component. Although the substitutions have little effect on the rate of the rapidly inactivating component (Table 1), V1 and V2 currents alter the relative magnitude of the noninactivating component. These changes are not due to a shift in voltage dependence, since they are also present at high membrane potentials (see Fig. 3B). Single-channel analysis of V2 (Fig. 4) indicates that the differences in macroscopic inactivation cannot be explained by an increase in mean open duration [0.81 ± 0.21 ms, $n = 6$, independent of

membrane potential, for V2; compared to 1.05 ms for 29-4 (ref. 17)]: the observed decrease in mean open duration suggests that the stability of the open-channel state in V2 is decreased. The experiment also shows that the mean number of bursts per depolarizing pulse in V2 (2.28 at $+20$ mV, 1.8 at $+40$ mV, and 1.92 at $+100$ mV) is not significantly affected by voltage. This is similar to wild-type 29-4 currents (17). However, for V2 there is an increase in the mean number of bursts per depolarizing pulse with openings; the mean value for V2 is 2.05 ± 0.21 ($n = 7$) whereas the value for wild-type 29-4 is 1.37 ± 0.14 ($n = 5$). Thus, an increased probability of channel reopening appears to account for the increase in the noninactivating component, perhaps by decreasing the stability of an inactivated state. One possibility is that amino

Table 1. Physiological properties of substitution mutants

Mutant	$V_{m1/2}$, mV	I_{ss}/I_{peak}	T1, ms	T2, ms	A1/(A1+A2)	n	$V_{h1/2}$, mV	$V_{h_{slope}}$, mV/e-fold	Charge number
Wild type	1 ± 5	0.14 ± 0.05	6.0 ± 1.1	26 ± 11	0.75 ± 0.03	15	-34 ± 1	3.7 ± 0.05	6.8
V1	100 ± 6	0.46 ± 0.07	5.3 ± 1.8	172 ± 185	0.65 ± 0.26	5	48 ± 4	17.4 ± 1.9	1.5
V2	69 ± 7	0.26 ± 0.01	5.4 ± 1.2	51 ± 22	0.84 ± 0.08	7	26 ± 3	11.0 ± 0.9	2.3
V3	-5 ± 2	0.11 ± 0.02	5.3 ± 0.2	—	1	3	-41 ± 2	3.2 ± 0.1	7.9
V4	-22 ± 3	0.13 ± 0.03	8.4 ± 1.5	—	1	5	-58 ± 6	3.6 ± 0.5	7.0
V5	-7 ± 7	0.12 ± 0.05	6.9 ± 1.1	—	1	5	-45 ± 4	4.0 ± 0.2	6.3
A3	-19 ± 3	0.08 ± 0.02	5.2 ± 0.6	—	1	5	-50 ± 4	3.1 ± 0.5	8.1
V2A3	32 ± 5	0.16 ± 0.02	9.1 ± 1.9	—	1	6	-9 ± 4	11.1 ± 3.0	2.3
V1 _{n-3}	3 ± 5	0.14 ± 0.05	7.0 ± 1.1	31 ± 9	0.76 ± 0.04	4	-32 ± 6	3.6 ± 0.3	7.0

$V_{m1/2}$ is the voltage at half-maximal conductance (cf. Fig. 3D). The ratio of peak current (I_{peak}) and steady-state current (I_{ss} , the current values remaining at the end of a 50-ms test pulse) was determined for test potentials standardized for each mutant at 30 mV above $V_{m1/2}$ (cf. Fig. 3A). Time constants of inactivation (T1 and T2) were obtained by fitting the decay of currents to a steady-state value with the double exponential function: $I_t/I_0 = [A1 \exp^{-t/T1} + A2 \exp^{-t/T2}]$ where I_t is the current at time t , I_0 is the extrapolated value of the peak current at $t = 0$, and $A1 + A2 = 1$. The data were obtained from currents during a 50-ms test pulse to 40 mV above $V_{m1/2}$ after a 1-s prepulse to -120 mV. Steady-state inactivation curves were fitted to a Boltzman distribution, $I/I_{max} = 1/[1 + e^{(V - V_{h1/2})/V_{hslope}}]$, where $V_{h1/2}$ is the midpoint of inactivation and V_{hslope} is expressed as the number of mV to produce an e -fold change in I/I_{max} . Prepulse inactivation curves were obtained as in Fig. 3 using test potentials of 30 mV except for V1 (100 mV), V2 (80 mV), and V2A3 (60 mV). Charge number is the number of apparent gating charges calculated as follows: charge = RT/FV_{hslope} . The number of oocytes from which the data in the preceding columns was obtained is n . Data are shown as mean \pm SD for the Sh construct indicated.

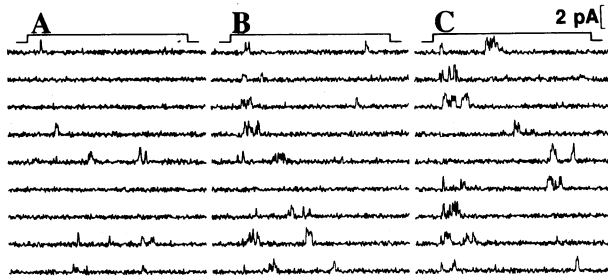


FIG. 4. Single channels in cell-attached patches (17) from an oocyte injected with V2 RNA. Nine representative sweeps at depolarizations to +20 mV (A), +40 mV (B), or +100 mV (C), from a holding potential of -100 mV, are shown. The depolarizing pulse (40 ms) is shown above each set of records. The minimum closed time used to distinguish bursts from individual openings was 2 ms. Each experiment consisted of 64 sweeps. The average of sweeps with no openings was used to subtract leak and uncompensated capacitive currents. Voltage steps were delivered every 5 s. The currents were low-pass filtered through an 8-pole Bessel filter at 2 kHz. Data were digitized at $50 \mu\text{s}$ per point.

acid residues in the heptad-repeat region are closely associated with the receptor for a blocking particle as proposed in some models of channel inactivation (5, 23). This receptor is thought to reside on or near the internal mouth of the pore. The alterations in both the probability of channel reopening and the mean open duration suggest that the conserved leucine-heptad-repeat region (thought to be located on the internal side of the membrane) may itself form a portion of the channel pore.

The effects of the mutations appear to define two functional classes for the heptad leucines. Class I mutations (V1 and V2) appear to impair transitions from closed to open states. They cause shifts of $V_{m1/2}$ and $V_{h1/2}$ to more positive potentials, decreases in the slopes of conductance-voltage and prepulse inactivation curves, and decreases in the extent of inactivation. Class II mutations (V3, A3, V4, and V5) appear to facilitate transitions from closed to open states, thereby causing shifts in $V_{m1/2}$ and $V_{h1/2}$ to more negative potentials with lesser effects on slope and the extent of inactivation. To determine how mutations in the various classes interact, we constructed the double mutant V2A3. The double mutant has $V_{m1/2}$, $V_{h1/2}$, and steady-state current values that are intermediate between those for the V2 and A3 single mutants (Table 1). In contrast, the slopes of the conductance-voltage (data not shown) and prepulse inactivation curves (Table 1) for the double mutant resemble those of V2, indicating that this effect is dominant and that the alterations in slope do not result indirectly from the voltages at which the channel opens or inactivates or from changes in steady-state current.

DISCUSSION

Hydrophobic Amino Acids Are Important in Stabilizing Open and Closed Conformations. Although leucine substitutions have little effect on other properties, some of the alterations in the conductance-voltage and prepulse inactivation curves are quite large. Our results show that conservative substitutions of hydrophobic amino acids in the S4 domain produce voltage shifts similar to, but of greater magnitude than, substitutions of the positively charged residues (6, 24–26). For example, the 100-mV shift in $V_{m1/2}$ and ≈ 5 times decrease in slope for the V1 mutant are striking. Furthermore, since these alterations occur without any net change in charge, the large decreases in slope (in V1 and V2) are particularly interesting. These slope changes may reflect large reductions in gating charge resulting from alterations in either the positioning of S4 charges (or dipole) relative to the

electric field vector or in the ability of subunits to reach their fully activated conformation. However, given the magnitude of slope differences it is difficult to explain in either of these terms how V1 and V2 channels could achieve open-channel conformations at all. One alternative possibility is that these slope changes may not reflect changes in charge movement of the voltage sensor. Furthermore, gating may require cooperative or other allosteric transitions; if residues in the leucine-heptad-repeat region, particularly L1 and L2, are critical in mediating the interactions underlying these allosteric transitions, then even conservative substitutions (V1 and V2) could alter activation and the apparent gating charge.

Our data are consistent with the proposal that the S4 domain (V1 and V2) is important in determining the observed voltage dependence of channel opening; however, mutations of leucines in S5, the next membrane-spanning domain (V4 and V5), and in the linker region between S4 and S5 (A3 and V3) also produce voltage shifts. In contrast, substitution of a valine for an isoleucine residue in S4, three residues upstream of L1 (V1n-3) and outside the defined leucine heptad repeat (see Fig. 1), results in no apparent changes in any of these properties (Table 1). Thus, not all hydrophobic amino acids in or near the S4 domain play a similar role to those in the leucine heptad repeat. Thus these data suggest that interactions mediated by heptad leucines are important in stabilizing conformational states of the channel and that these interactions may strongly influence the transduction of charge movement into channel opening and closing. Leucines in the heptad repeats of Na^+ and Ca^{2+} channels may play similar roles. For example, in the rat IIa Na^+ channel, substitution of L1 (in the second homology domain) by a phenylalanine results in a voltage shift of +25 mV whereas substitution of six other residues, including charged or transmembrane residues, had no effect (24).

Significance of the Heptad Repeat. The asymmetry of effects in the two classes of mutations may indicate that the first two and the last two or three leucines in the motif stabilize different conformational states of the channel. This is consistent with the proposal that the leucines are located in two separate (possibly transmembrane) domains. Given the fact that the V1 and V2 mutations have similar effects and the frequent occurrence of helical transmembrane segments, our results suggest that L1 and L2 may be aligned along one face of a helix to interact with other channel structures that stabilize conformational states of S4. The similar effects of the V4 and V5 mutants also suggest the possibility of helical structure in this portion of the S5 domain. In the *Sh*⁵ mutation, substitution of a phenylalanine located between L4 and L5 by isoleucine produces a voltage shift in the opposite direction of V4 and V5 (19, 27); this residue would be located on the opposite face of an α -helix from that of L4 and L5. It will be interesting to correlate the mutagenic effects of other residues in and around the heptad-repeat region as a function of the helical face on which they may lie.

Two issues that remain unclear are: (i) why L3 and the 7-residue periodicity in the cytoplasmic linker between the S4 and S5 segments are highly conserved in voltage-gated ion channels and (ii) why conservative hydrophobic substitutions in a putative transmembrane domain (V1 and V2) have such large effects on the conductance-voltage and prepulse inactivation curves. In the DNA-binding leucine-zipper proteins, dimerization mediated by the heptad-repeat region appears to be a contiguous coiled coil association of two α -helices (28); dimerization takes place largely through the buried leucine (hydrophobic) residues along one face of the respective helices. Helical projections of the heptad-repeat region of *Drosophila* Shaker (*Sh*), *Sh* family members, and Na^+ channels (Fig. 5) demonstrate that the arms of one face of the helix, including the leucine arm, are conserved whereas the arms of the opposite face are not. Although a

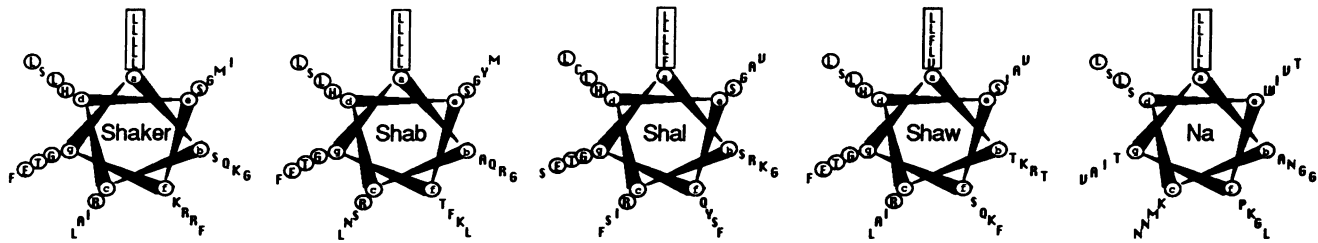


FIG. 5. Helical projections of the indicated sequences (aligned in Fig. 1). Residues of the heptad repeat are boxed and residues that are conserved among all of the K^+ channel sequences and the indicated sequence are circled. Arms a, d, and g are well conserved among all published K^+ channel sequences. Adjacent arms a and d, which could potentially mediate coiled-coil interactions, are well conserved even in Na^+ channel sequences.

contiguous helix containing the five leucines of the repeat is inconsistent with the positioning of both the S4 and S5 domains perpendicular to the membrane, it is striking that a specific type of structural organization, with an approximate 3.5-residue periodicity, has been conserved in this region in many species and many types of voltage-dependent ion channels. One possibility is that the portion of the S4 domain that contains L1 and L2 may not be located in the membrane in all channel conformational states; residues located between the charged residues in this portion of S4 are less hydrophobic than those in the remaining portion of S4 supporting this possibility. In addition, the large voltage shifts and slope alterations observed in V1 and V2 also suggest that this portion of the S4 domain may be in an aqueous environment since the energetics of leucine-mediated hydrophobic interactions might be relatively large in such an environment in comparison to the membrane interior. It is possible that they lie in or near the aqueous environment of the channel pore.

Substitution of heptad leucines resulted in alterations in the "effective" voltage dependence of channel opening. This is consistent with the proposal that voltage-dependent conformational changes of gating-charge movement may be transduced through subunit interactions mediated by the leucine-heptad-repeat region into opening of the channel pore (9). In addition, alterations in activation and in the stability of the channel pore were observed, suggesting that the conserved heptad-repeat region, itself, may be involved in determining a portion of the channel pore.

We thank H. A. Lester, N. Davidson, X. C. Yang, and R. Dunn for kindly providing rat IIA Na channel RNA; and H. A. Lester for oocytes; D. Rees and T. Kouzarides for helpful discussions; W. N. Zagotta and R. Aldrich for providing a manuscript prior to publication; and R. McMahon for expert technical assistance. This research was supported by U.S. Public Health Service Grants NS21327 and GM42824 to M.A.T., GM26976 to B.R., NS28135 to L.E.I., and GM29836 to H. A. Lester.

- Iverson, L. E., Tanouye, M. A., Lester, H. A., Davidson, N. & Rudy, B. (1988) *Proc. Natl. Acad. Sci. USA* **85**, 5723–5727.
- Stuhmer, W., Ruppersburg, J. P., Schroter, K. H., Sakman, B., Stocker, M., Giese, K. P., Perschke, A. & Pongs, O. (1989) *EMBO J.* **8**, 3235–3244.

- Wei, A., Covarrubias, M., Butler, A., Baker, K., Pak, M. & Salkoff, L. (1990) *Science* **248**, 599–603.
- Hodgkin, A. L. & Huxley, A. F. (1952) *J. Physiol. (London)* **117**, 500–544.
- Armstrong, C. M. (1981) *Physiol. Rev.* **61**, 644–683.
- Stuhmer, W., Conti, F., Suzuki, H., Wang, X., Noda, M., Yahagi, N., Kubo, H. & Numa, S. (1989) *Nature (London)* **339**, 597–603.
- Numa, S. (1987) *Biochem. Soc. Symp.* **52**, 119–143.
- McCormack, K., Lin, J. W., Iverson, L. E. & Rudy, B. (1990) *Biochem. Biophys. Res. Commun.* **171**, 1361–1371.
- McCormack, K., Campanelli, J. T., Ramaswami, M., Mathew, M. K., Tanouye, M. A., Iverson, L. E. & Rudy, B. (1989) *Nature (London)* **340**, 103.
- Kamb, A., Tseng-Crank, J. & Tanouye, M. A. (1988) *Neuron* **1**, 421–430.
- Ramaswami, M., Gautam, M., Kamb, A., Rudy, B., Tanouye, M. A. & Mathew, M. K., *Cell. Mol. Neurosci.*, in press.
- Tanabe, T., Takeshima, H., Mikami, A., Flockerzi, V., Takahashi, H., Kangawa, K., Kojima, M., Matsuo, H., Hirose, T. & Numa, S. (1987) *Nature (London)* **328**, 313–318.
- Kouzarides, T. & Ziff, E. (1988) *Nature (London)* **336**, 646–651.
- Scheurmann, M., Neuberg, M., Hunter, J. B., Jenuwein, T., Ryseck, R. P., Bravo, R. & Muller, R. (1989) *Cell* **56**, 507–516.
- Buckland, R. & Wild, F. (1989) *Nature (London)* **338**, 547.
- White, M. K. & Weber, M. J. (1989) *Nature (London)* **340**, 103.
- Iverson, L. E. & Rudy, B. (1990) *J. Neurosci.* **10**, 2903–2916.
- Gisselman, G., Sewing, S., Madsen, B. W., Mallart, A., Angrand-Petit, D., Muller-Holtkamp, F., Ferrus, A. & Pongs, O. (1989) *EMBO J.* **8**, 2359–2364.
- Gautam, M. & Tanouye, M. A. (1990) *Neuron* **5**, 67–73.
- Zagotta, W. N. & Aldrich, R. W. (1990) *J. Gen. Physiol.* **95**, 29–60.
- Yeh, J. Z., Oxford, G. S., Wu, C. H. & Narahashi, T. (1976) *J. Gen. Physiol.* **68**, 519–535.
- Meves, H. & Pichon, Y. (1977) *J. Physiol. (London)* **268**, 511–532.
- Hoshi, T., Zagotta, W. N. & Aldrich, R. W. (1990) *Science* **250**, 533–538.
- Auld, V. J., Goldin, A. L., Krafte, D. S., Catterall, W., Lester, H. A., Davidson, N. & Dunn, R. (1990) *Proc. Natl. Acad. Sci. USA* **87**, 323–327.
- Papazian, D. M., Timpe, L. C., Jan, Y. N. & Jan, L. Y. (1989) *Soc. Neurosci. Abstr.* **15**, 337.
- McCormack, K., Ramaswami, M., Mathew, M. K., Tanouye, M. A., Iverson, L. E., McCormack, T. & Rudy, B. (1989) *Soc. Neurosci. Abstr.* **15**, 337.
- Zagotta, W. N. & Aldrich, R. W. (1990) *J. Neurosci.* **10**, 1799–1810.
- O'Shea, E. K., Rutkowski, R. & Kim, P. S. (1989) *Science* **243**, 538–542.